

Antimicrobial polymers: Antibacterial efficacy of silicone rubber–titanium dioxide composites

Betiana Felice^{1,2}, Vera Seitz³, Maximilian Bach³,
Christin Rapp³ and Erich Wintermantel³

Journal of Composite Materials
2017, Vol. 51(16) 2253–2262
© The Author(s) 2016
Reprints and permissions:
sagepub.co.uk/journalsPermissions.nav
DOI: 10.1177/0021998316668984
journals.sagepub.com/home/jcm



Abstract

Control and reduction of microorganism infections in high-risk environments is up to date a challenge. Traditional techniques imply several limitations including development of antibiotics resistance and ecotoxicity. Then, polymers functionalized with photocatalysts arise as a promising solution against a broad spectrum of microorganisms found at, e.g. sanitary, food, and medical environments. Here, we present silicone rubber–TiO₂ composites as novel antibacterial polymers. Four different types of composites with different TiO₂ contents were produced and analyzed under UV irradiation and dark conditions in terms of particle distribution, chemical composition, photocatalytic activity, wettability, and antibacterial efficacy against *Escherichia coli*. Under UV irradiation, antibacterial sensitivity assay showed a 1000 times reduction of colony forming units after 2 h of light exposure so that the antibacterial ability of silicone–TiO₂ composites was proved. Photocatalytic activity assessment suggested that reactive oxygen species induced by photocatalytic reaction at TiO₂ particles are the main cause of the observed antibacterial effect. Scanning electron microscopy indicated no topographical damage after UV exposure. In addition, chemical analysis through Raman and X-Ray photoelectron spectroscopies demonstrated the stability of the silicone matrix under UV irradiation. Hence, the current work presents silicone–TiO₂ composites as stable nonspecific antibacterial polymers for prevention of infections at multiple high-risk environments.

Keywords

Antibacterial polymers, silicone rubber, titanium dioxide (TiO₂), composites, antibacterial activity

Introduction

Bacterial infections are up to date a primary human death cause. In consequence, multiple antibacterial solutions have been developed in order to prevent microorganism attachment and growth in environments with high risk of infection. So far disinfectants such as hypochlorite, hydrogen peroxide, or quaternary ammonium compounds are repeatedly applied, but their short-term effect and environmental safety limit their use.^{1–4} Then, antibacterial polymers arise as promising materials for long-term effective infection prevention at, e.g. sanitary facilities, food packaging, hospital environments, and water purification systems.^{5–9}

Nowadays common antibacterial polymers are based on either biocidal polymers or silver compounds. The former are mostly polymers with uniform mechanical properties whose chains have intrinsic antibacterial activity through, e.g. the addition of quaternary ammonium compounds or halogenic components which in

contact with the surface of microorganisms induce cell destruction.^{1,10} The latter primarily comprise polymers coated with silver-based compounds which in solution release silver ions already known for their fast antibacterial response, biocompatibility and high antibacterial effectiveness against a broad spectrum of microorganisms.^{11–14} Nevertheless, the slow response and no biocompatibility of most biocidal polymers as

¹Laboratorio de Medios e Interfases, Departamento de Bioingeniería, Facultad de Ciencias Exactas y Tecnología, Universidad Nacional de Tucumán, Tucumán, Argentina

²Instituto Superior de Investigaciones Biológicas, CONICET, Tucumán, Argentina

³Institute of Medical and Polymer Engineering, Technische Universität München, Garching, Germany

Corresponding author:

Betiana Felice, Departamento de Bioingeniería, Facultad de Ciencias Exactas y Tecnología, Universidad Nacional de Tucumán, Av. Independencia 1800 CP4000, Tucumán, Argentina.
Email: betiana_felice@yahoo.com.ar

well as frequent allergic reactions and ecological problems caused by silver ions lead to photocatalytic compounds as a solution for safe antibacterial polymers.^{15–17} Among them, titanium dioxide (TiO₂) emerges as a promising antibacterial agent for functionalization of polymers.

TiO₂ is a metal oxide semiconductor with a desirable photocatalytic efficiency, chemical stability, low toxicity, and acceptable cost.^{18,19} Antibacterial activity of TiO₂ is based on its intrinsic ability to induce the production of reactive oxygen species (ROS) in the presence of oxygen and water under UV irradiation. ROS cause oxidative degradation of biological structures followed by microorganism death.²⁰ Therefore, TiO₂ is able to exert its antibacterial effect in close proximity to target microorganism without biocide release.^{20,21}

Up to date, TiO₂ as antibacterial agent has been mainly applied as coating compound of, e.g. polyester fabrics, polyetheretherketone (PEEK), and polyurethane complexes.^{22–24} Although TiO₂ coatings demonstrated high bactericidal activity and efficiency, their high costs, inhomogeneous mechanical properties and demanding technology necessary for surface treatments lead to TiO₂-based composites as an alternative.¹⁵ Previous works of this group assessed polypropylene, polyamide 6, and polyamide 12 as thermoplastic matrices for TiO₂-based antibacterial composites.^{25,26} Despite the studies demonstrated an intense antibacterial activity under UV irradiation, all matrices showed strong degradation within the first 24 h of UV exposure, with clear evidence of chain scission and topographical damage. In order to avoid aforementioned drawbacks, the primary aim of this work was to develop and evaluate thermoset–TiO₂ composites against *Escherichia coli* under UV irradiation. Medical-grade silicone rubber was chosen as model polymer matrix given that its exceptional chemical and thermal stability in addition to its biocompatibility considering future applications at sanitary, medical, and food environments.²⁷

Experimental section

Materials

Medical-grade silicone rubber tested according to USP Class VI (Silpuran 2430[®], room temperature vulcanization, two-components system) was supplied from Wacker Chemie AG (Germany) whereas nanostructured TiO₂ powder (Aeroxide[®] P25 TiO₂) with an average primary particle size of 21 nm was kindly provided by Evonik Degussa GmbH (Germany). Methylene blue (MB) for photocatalytic activity assessment and Tween 80[®] used during microbiological assay were acquired from Merck (Germany). For antibacterial activity evaluation, samples were tested against *E. coli*

(Wildtype K12, DSM 498). Agar-agar, yeast extract, tryptone/peptone, and salts were supplied by Carl Roth GmbH + Co. KG (Germany).

Samples preparation

Composite samples were prepared by manual blending of silicone rubber with TiO₂ powder. In short, a specific amount of TiO₂ powder was blended with component A of the silicone rubber system until a homogeneous compound was obtained. Subsequently, component B was added and uniformly incorporated to the former compound. Finally, the obtained composite was deaerated for 5 min under vacuum and then poured onto an aluminum mold. Silicone rubber vulcanization was performed at 200°C for 45 min followed by a heat treatment at 100°C for 4 h, in line with silicone supplier instructions. Round platelets of 15 mm in diameter and 0, 2, 5, and 10 w/w% of TiO₂ were prepared.

Before every characterization assay, samples were thoroughly washed with 70% isopropanol, rinsed with distilled water, dried, and autoclaved at 121°C for 15 min.

Scanning electron microscopy

Surface topography as well as dispersion of TiO₂ particles in silicone rubber matrix was characterized using a scanning electron microscope (Hitachi S3500-N, Japan) operating at an accelerating voltage of 30 kV and fitted with an energy dispersive X-ray spectroscopy (EDX) accessory for further composition analysis. The samples were sputter coated with gold before SEM imaging. Micrographs were taken at low and high magnification in order to have a detailed overview of different batches of samples prepared during this study. Twenty-four-hour-UV irradiated and non-UV-irradiated samples of pure silicone and silicone–TiO₂ composites were analyzed.

Elemental and molecular analysis

Chemical analysis of 24 h-UV-irradiated and non-UV-irradiated samples of pure silicone (0% TiO₂) and silicone–TiO₂ (10% TiO₂) was performed through X-ray Photoelectron Spectroscopy (XPS) and Raman spectroscopy. XPS spectra were acquired with a Leybold-Heraeus LHS 10 XPS system in ultra-high vacuum at a pressure below 5×10^{-8} mbar hosting a nonmonochromatic MgK α -source (1253.6 eV). XPS samples were fixed on the specimen holder with a vacuum-compatible copper foil adhesive tape. The spectra were recorded at a constant pass energy mode set to 100 eV and a full width at half maximum of ~ 0.1 eV. The C 1s (284.38 eV) peak corresponding to adventitious carbon was used as energy reference to compensate

energy shifts due to charging. Shirley backgrounds were subtracted from all spectra and core level spectra were fitted by Gaussian/Lorentzian functions.

For Raman spectroscopy, a Senterra Raman spectrometer (Bruker Corporation, USA) equipped with a 40 mW 488 nm laser and 50× magnification objective was used. Besides baseline correction through Rubber Band method, each Raman spectra was recorded with 1 s of integration time and 100 coadditions. Three specimens per sample were analyzed.

Photocatalytic activity assessment

Photocatalytic activity of pure silicone and silicone–TiO₂ samples was evaluated by means of MB discoloration assay according to DIN 52980.²⁸ Briefly, specimens were arranged in 24-multiwell plates filled with 2 ml of 10 μmol aqueous MB solution. Subsequently, one group of samples was placed under a UV lamp (365 nm, 15 W, UV-A A15, Vilber, France) and continuously irradiated for 4 h whereas a second group was kept under dark conditions for the same amount of time. Then, MB changes were monitored through light absorbance variations at 620 nm, which were registered by an UV–Visible spectrometer (Multiscan FC, Thermo Scientific, Germany). The relative absorbance of MB was calculated with following equation

$$\text{Methylene Blue Relative Absorbance (\%)} = \frac{\text{Ref}_{\text{abs}} - \text{S}_{\text{abs}}}{\text{Ref}_{\text{abs}}} \times 100$$

where Ref_{abs} is the absorbance of MB solution not in contact with samples and S_{abs} is the absorbance of MB solution in contact with silicone and silicone–TiO₂ samples. Positive values of relative absorbance indicate prevalence of MB reduction whereas negative values indicate prevalence of MB oxidation. Therefore, as TiO₂ tends to reduce MB molecule, positive values of relative absorbance indicate predominance of TiO₂ photocatalytic activity.

Photocatalysts as TiO₂ normally undergo a deactivation process induced by UV irradiation. Thus, in order to assess such photocatalyst deactivation, samples were continuously preirradiated with UV light during specific periods of time under dry conditions. Subsequently, samples were subjected to above-mentioned MB protocol in order to measure remaining photocatalytic activity.

Wettability

The effect of TiO₂ particles on wettability was assessed through water contact angle analysis according to sessile droplet method under ambient conditions.²⁹ One group of samples was irradiated with UV light for

24 h whereas a second group was kept under dark conditions for the same amount of time. Two microliter droplets of deionized water were pumped onto samples surfaces and contact angle was further obtained by analysis system OCA 20 (Dataphysics Instruments, Germany). Measurements were performed three times per sample and average values were reported.

Antibacterial sensitivity assay

Antibacterial effect of silicone and silicone–TiO₂ samples was evaluated against *E. coli* according to DIN 13697.³⁰ Samples were inoculated with 10 μl of 3.5×10^8 CFU/ml *E. coli* in PBS-0.1% Tween[®] suspension. Then, specimens were irradiated with UV light (365 nm) for 2 h at room temperature in order to induce photocatalytic response and subsequently thoroughly washed with 1 ml of PBS-0.1% Tween[®]. Fifty microliters of former suspension was pipetted and dissolved in 450 μl of fresh PBS. These steps were repeated with inoculated specimens kept under dark conditions for 2 h. After that, 100 μl of each bacterial PBS suspension of each specimen was streaked and uniformly spread over LB-Bouillon agar in Petri dishes which were then incubated for 24 h at 37°C. Finally, colony forming units (CFU) were counted and evaluated.

Results and discussion

Surface topography

Figures 1 and 2 show SEM micrographs of pure silicone and silicone–TiO₂ samples non-UV irradiated and UV irradiated, respectively. An overlap of Ti-EDX mapping with SEM pictures of non-UV-irradiated samples is displayed, which clearly suggests a uniform distribution of TiO₂ particles at all samples coexisting with agglomerates of around 20 μm possibly produced by defective manual stirring. EDX mapping also indicates that the higher the TiO₂ content, the higher the number of agglomerates detected. However, although such presence of multiple agglomerates, SEM micrographs reveal almost no exposed TiO₂ agglomerates at samples surface. Additionally, UV irradiation seems to have no noticeable effect on surface topography in accordance with Figures 1 and 2. Such composite response contrasts with previous results of this group, which demonstrated a strong observable degrading effect of UV light on most thermoplastics assessed as polymer matrices.²⁶

Elemental and molecular analysis

XPS survey spectra of 0% TiO₂ and 10% TiO₂ samples are shown in Figure 3. Strikingly, survey spectra as well as core level spectra of 10% TiO₂ specimens lack of

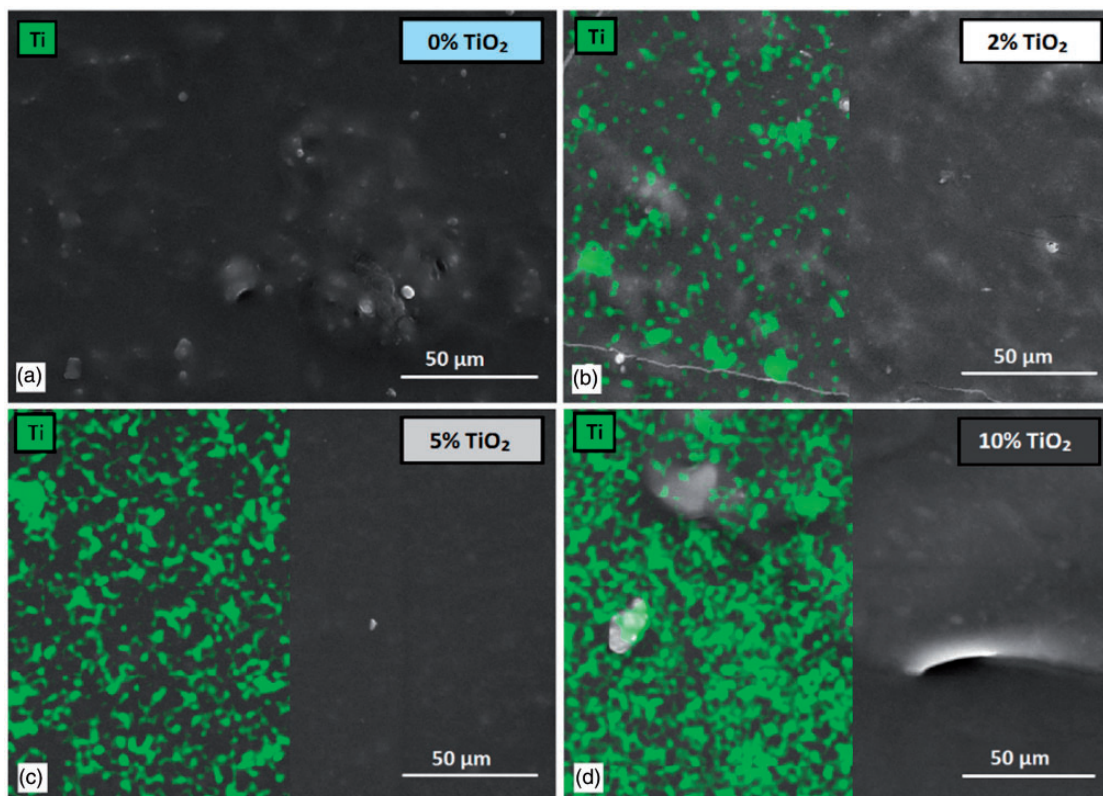


Figure 1. SEM micrographs overlapped with EDX mapping of titanium (green dots) of (a) 0% TiO₂, (b) 2% TiO₂, (c) 5% TiO₂, and (d) 10% TiO₂ samples with no previous UV irradiation.

most intensive TiO₂ photoelectron lines which normally are found at 458.5 eV (Ti 2p_{3/2}) and 464 eV (Ti 2p_{1/2}). Hence, these results suggest the absence of TiO₂ particles at samples surface within the first 10 nm according to average analysis depth of XPS.³¹

Furthermore, even though SEM analysis did not prove any topographical change before and after UV irradiation, XPS core level spectra of Si 2p peak (Figure 4) contrastingly demonstrate silicone rubber oxidation, which is apparently caused by UV light and ROS induced by TiO₂-photocatalytic reaction. Figure 4 shows Si 2p peaks of 0% TiO₂ and 10% TiO₂ samples before and after 24 h of UV irradiation. As it can be seen in Figure 4, Si 2p peaks of pure silicone as well as 10% TiO₂ samples are shifted to higher binding energies after UV irradiation. Such peak shifting indicates that oxidation of silicone rubber takes place, a phenomena also observed after laser irradiation of silicone rubber samples during Armyanov et al. studies.³² However, while pure silicone Si 2p peak is shifted +0.05 eV, a +0.9 eV shift is recorded at 10% TiO₂ samples after irradiation suggesting a stronger oxidation. Deconvolution after curve fitting explains this effect. It is known that the energy of Si 2p peak is determined by Si position in the polymer chain as well as its oxidation degree. When Si atoms of silicone rubber are bound to two

oxygen atoms (Si(-O)₂), Si 2p peak is at 101.8 eV; three oxygen atoms (Si(-O)₃), 102.6 eV; and four oxygen atoms (Si(-O)₄), 103.3 eV.^{32,33} As in crosslinked silicone chains many Si-oxidation states could be found, Si 2p peak results in the convolution of Si(-O)_x-associated peaks. The analysis of deconvolved curves first indicates that Si 2p peak is resolved into two main components (Figure 4): Si(-O)₂ at 101.7 eV and Si(-O)₃ at 102.6 eV. Si(-O)₄ at 103.3 eV remains negligible for almost all samples except irradiated 10% TiO₂ specimens. After UV irradiation there is a clear increase of the area under Si(-O)₃ deconvolved curves from 8 to 26% at 0% TiO₂ samples, and from 13 to 36% at 10% TiO₂ samples, indicating a clear oxidation of silicone rubber. Nevertheless, as after irradiation no intensity variation of Si(-O)₂ peak is recorded, it can be assumed that oxygen-silicon-oxygen bondings at the main chain were not broken so that exceptional stability of silicone rubber under UV irradiation was maintained. Hence, silicone rubber oxidation might be primarily attributed to split of methyl-side groups followed by oxygen bonding to remaining Si to produce an enrichment in nonstoichiometric oxygen deficient silicone chain.³² It must be noted that after irradiation Si(-O)₃ is significantly more intensive for 10% TiO₂ than for 0% TiO₂ samples, which suggests that ROS induced by

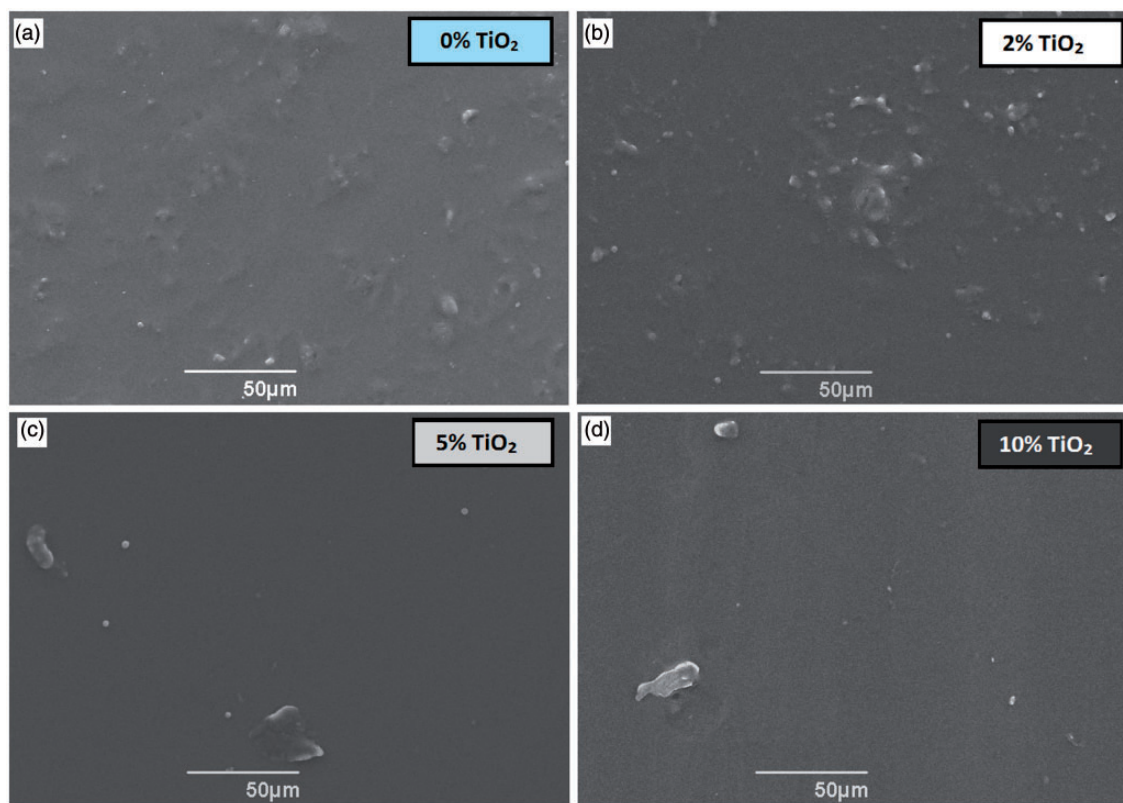


Figure 2. SEM micrographs of (a) 0% TiO₂, (b) 2% TiO₂, (c) 5% TiO₂, and (d) 10% TiO₂ samples previously irradiated with UV light for 24 h.

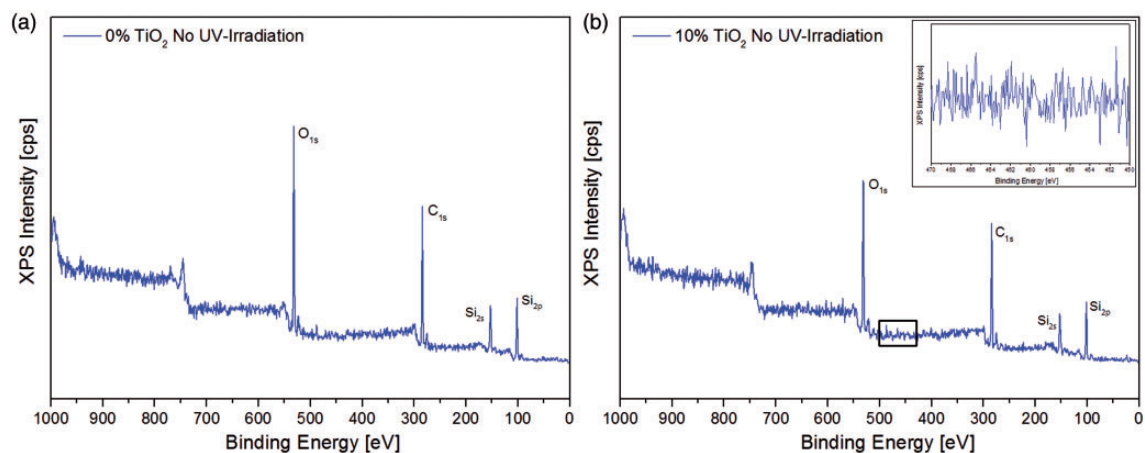


Figure 3. XPS survey spectra of (a) 0% TiO₂ (pure silicone) and (b) 10% TiO₂ samples with no UV irradiation. Carbon and oxygen and silicon photoelectron lines are tagged. No titanium photoelectron lines are detected at survey spectra as well as at core level spectra between 450 and 470 eV (inset figure).

photocatalytic reaction at TiO₂ intensify oxidation of silicone rubber.

Figure 5 shows Raman spectra of 0 and 10% TiO₂ samples before and after UV irradiation while Table 1 specifies main bands observed as well as their corresponding vibration mode. Typical silicone rubber bands

are present at both spectra, whereas characteristic bands of TiO₂ P25 at 513 and 637 cm⁻¹ arise at after incorporation of TiO₂ particles. Both spectra lack of new bands or band shifting after UV irradiation, which demonstrates the absence of strong chemical modifications. Though, after UV irradiation, it must

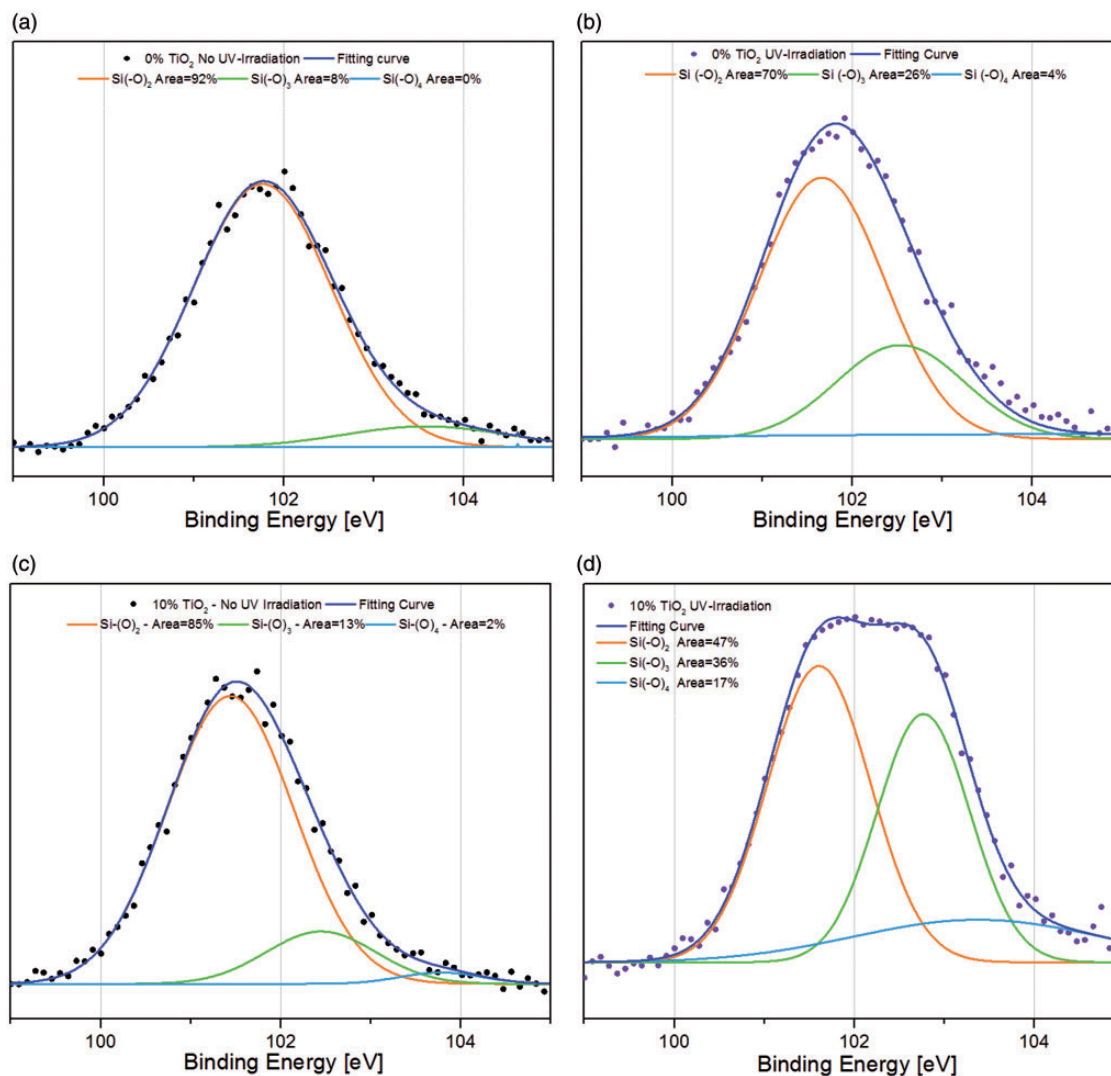


Figure 4. Curve fitting of XPS spectra of Si 2p for 0% and 10%TiO₂ samples not irradiated with UV light (a, c); and 0 and 10% TiO₂ samples after 24 h of UV irradiation (b, d). The blue line is the fitting curve. Orange line Si(-O)₂ 101.8 eV, green line Si(-O)₃ 102.6 eV, and light blue line Si(-O)₄ 103.3 eV. Areas under the curves are indicated in the boxes. For color interpretation, the reader is referred to the web version of this article.

be noted that the intensity of all silicone-related bands is diminished. Such effect is greater at 489 cm^{-1} (O–Si–O stretching) and 710 cm^{-1} (Si–C). These variations seem to be more pronounced for 10% TiO₂ samples where, after UV irradiation, decreases of 24 and 22% at 489 and 710 cm^{-1} bands, respectively, are two times bigger than intensity decreases undergone by the same bands at pure silicone samples. Therefore, it can be further assumed that silicone rubber oxidation by UV light and ROS induces Raman intensity decrease of silicone-related bands.

Photocatalytic activity

Given that antibacterial effects of silicone–TiO₂ composites might be principally due to oxidative

degradation by ROS, photocatalytic activity was measured through MB discoloration assay at nonirradiated and irradiated samples. Many authors report that MB is mainly reduced by TiO₂ under UV irradiation, which is observed as solution discoloration.^{36,37} Results are shown in Figure 6 where it can be clearly seen that, without UV light, samples lack of photocatalytic activity. Contrastingly, under UV irradiation, MB is discolored by composite samples where such effect linearly increases with higher contents of TiO₂ particles, therefore suggesting ROS as primary cause of MB discoloration.

It must be particularly noted that even though ROS might be the main cause of MB discoloration, final relative absorbance is further influenced by strong absorption of MB on silicone rubber in addition to

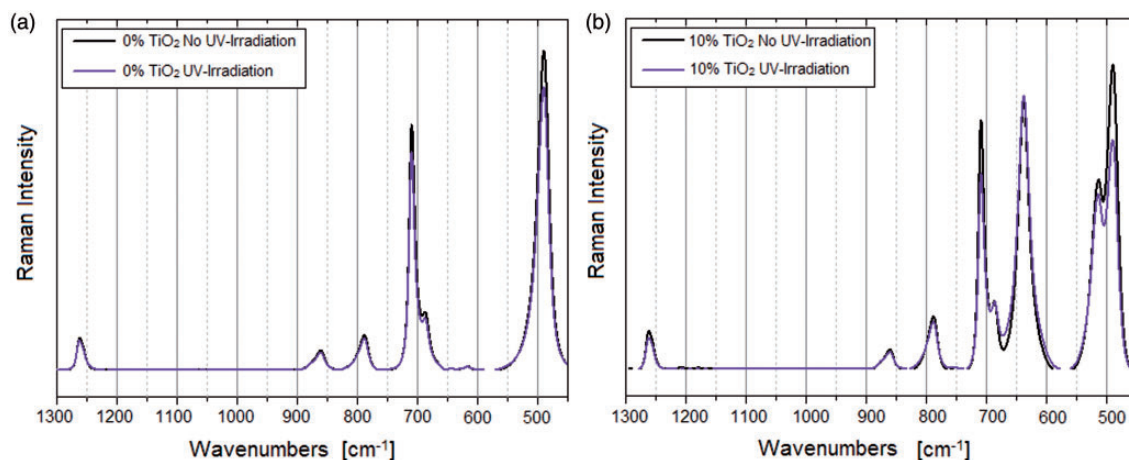


Figure 5. Raman spectra of (a) 0% TiO₂ and (b) 10% TiO₂ samples irradiated and nonirradiated with UV light. Spectra were obtained with a laser operating at λ 488 nm. For color interpretation, the reader is referred to the web version of this article.

Table 1. Raman analysis. Raman bands at 0% TiO₂ and 10% TiO₂ samples nonirradiated and irradiated with UV light.^{34,35}

0% TiO ₂		10% TiO ₂		Vibrational mode
Wavenumbers (cm ⁻¹) no UV Irradiation	Wavenumbers (cm ⁻¹) UV irradiation	Wavenumbers (cm ⁻¹) no UV irradiation	Wavenumbers (cm ⁻¹) UV irradiation	
1263	1263	1263	1263	CH sym. bending
861	861	861	861	CH ₃ sym. rocking
788	788	788	788	CH ₃ sym. rocking
710	710	709	709	Si-C sym. stretch
687	687	689	686	Si-CH ₃ sym. rocking
645	645	–	–	Si-CH ₃ sym. rocking
–	–	637	637	E _g (TiO ₂ Anatase)
616	616	–	–	Si-CH ₃ sym. rocking
–	–	513	513	E _{1g} (TiO ₂ Anatase)
489	489	489	489	Si–O–Si stretching

oxidation of leuco-MB, the reduced form of MB molecule, by UV light. Latter phenomenon is likely to mask real photocatalytic activity which might be higher without such influence, as occurs with 2% TiO₂.^{38,39}

Photocatalysts as TiO₂ normally undergo a deactivation process over time under UV irradiation according to many works.^{40,41} To study this phenomena, samples were deactivated through preirradiation with UV light and subsequently subjected to ordinary MB assay in order to evaluate remaining photocatalytic activity of silicone–TiO₂ composites along the time and to determine optimal analysis time for further characterizations. Results shown in Figure 7 clearly demonstrate deactivation of the photocatalyst. Due to aforementioned oxidation of leuco-MB by UV light, a proper quantitative analysis cannot be performed.

Nevertheless, it can be observed that 5 and 10% TiO₂ samples lose ~50% of apparent initial photocatalytic activity after 1 and 2 h of UV preirradiation, respectively, whereas after 24 h such decrease reaches values around 90%. Thus, to ensure photocatalytic activity at TiO₂ particles during characterization of samples, duration of assays was restricted to 24 h of UV irradiation.

It is worth to mention that UV light power applied in this work was around 50 times more intensive than UV light power at normal environments, so that longer photoactive times might be expected under ordinary lighting conditions.

Wettability

Water contact angle in function of TiO₂ content of irradiated and nonirradiated samples is shown in

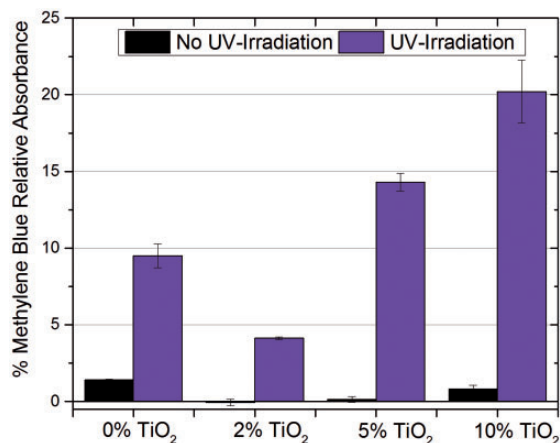


Figure 6. Methylene blue relative absorbance versus % TiO₂ (n = 5). Maximal methylene blue discoloration is reached with 10% TiO₂.

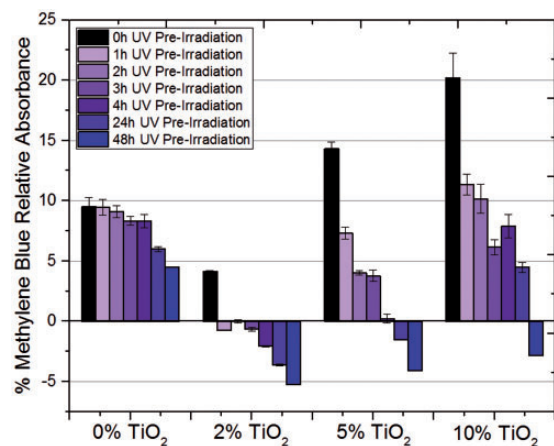


Figure 7. Photocatalyst deactivation. Methylene blue relative absorbance versus % TiO₂ is plotted (n = 5). Bar colors indicate UV preirradiation time before normal methylene blue assay. For color interpretation, the reader is referred to the web version of this article.

Figure 8. As it can be seen, nonirradiated samples undergo a contact angle decrease from 111° to 103° with higher contents of TiO₂, whereas samples UV irradiated demonstrate an increase of contact angle with respect to nonirradiated ones. Both phenomena must be explained separately.

As it was previously proved through XPS, silicone rubber is oxidized by UV light and ROS. Such oxidation usually induces contact angle decrease at silicone rubber, according to what many authors report.^{42–44} However, it must be noted that decreases recorded up to date imply the use of extreme conditions in order to produce contact angle reductions, which are primarily due to significant increments of Si(O)₄. For instance,

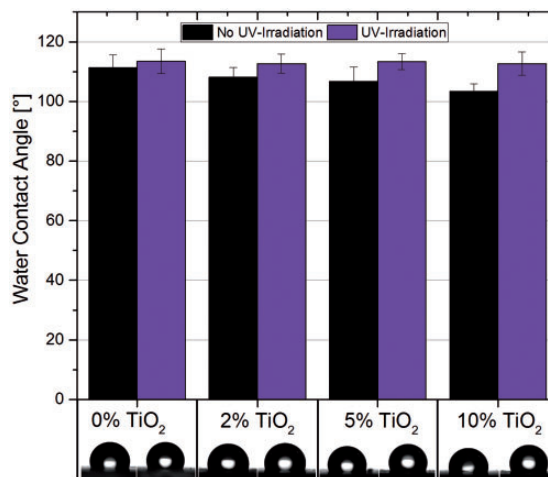


Figure 8. Water contact angle versus w/w% TiO₂ (n = 3, i = 3).

Youn et al. reported a 10° water contact angle decrease after 5000 h of exposure to UV light λ 313 nm, whereas Olah et al. observed a reduction by 4° after 36 h under UV light λ 185 nm and 55 ppm ozone atmosphere.^{42,44} Both studies also showed XPS spectra with Si(O)₄ peaks at \sim 103.3 eV with intensities and areas of the same order of magnitude as Si(O)₂ peak which indicated a marked oxidation of silicone. Then, as in this work no extreme conditions were applied in addition to the lack of Si(O)₄ peaks at 103.3 eV after UV irradiation, it can be assumed that any variation of contact angle was not caused by oxidation of silicone rubber.

In order to obtain droplet images, contact angle measurement necessarily implies the use of a light source which, besides visible light wavelengths, emits a portion of UV-A spectra. Given that the relatively high quantum efficiency of TiO₂, few photons with enough energy emitted by the light source of the device are suitable to excite electrons at TiO₂ particles.⁴⁵ Therefore, ROS are subsequently produced during the contact angle measurement and, therefore, induce the observed temporal hydrophilic effect at non-irradiated samples. Then, when considering contact angle dependency on TiO₂ content at nonirradiated samples as shown in Figure 8, in addition to the absence of such response after 24 h of UV irradiation, it can be concluded that contact angle variations are primarily caused by ROS which after 24 hours of UV irradiation are not anymore detected due to aforementioned intrinsic photocatalyst deactivation process.

Antibacterial sensitivity assay

Figure 9 shows the results of antibacterial sensitivity assay, which clearly demonstrates that silicone-TiO₂ composites have antibacterial activity under UV light

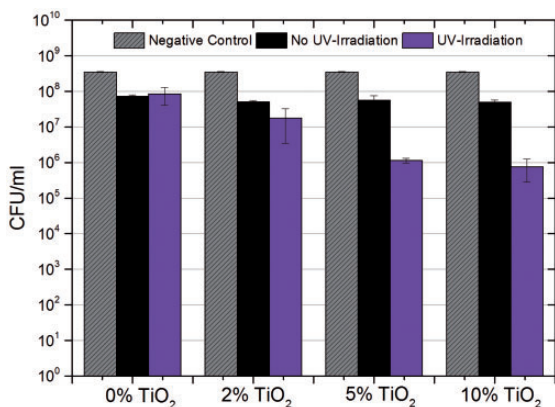


Figure 9. CFU/ml versus w/w% TiO₂ (n = 3). Maximal antibacterial effect was reached at 10% TiO₂.

and that increased amounts of TiO₂ particles lead to a lower surviving rate of bacteria. As it can be seen, with 10% of TiO₂ content 1000 times reduction of CFUs per milliliter was obtained after 2 h of incubation under UV irradiation. Contrastingly, results under dark conditions indicate less than 10 times reduction of CFUs per milliliter at all samples proving the absence of photo-induced antibacterial activity in addition to a slight intrinsic antibacterial activity of silicone rubber. Hence, it can be assumed that silicone–TiO₂ composites exert antibacterial effect under UV irradiation and that such effect is primarily due to ROS produced by photocatalytic reaction at TiO₂ particles.

Conclusion

Antibacterial polymers are nowadays an effective solution against recurrent infections. Silicone–TiO₂ composites arise as a promising and technologically not demanding approach against a broad spectrum of microorganisms. In this work it was shown that ROS released from material bulk under UV light exerted an antibacterial effect against *E. coli* for specific periods of time. This effect was shown to be more intensive with higher contents of TiO₂. Furthermore, silicone rubber matrix demonstrated to be resistant against UV light and ROS. Therefore, our study clearly suggests silicone–TiO₂ composites as exceptionally stable antibacterial polymers.

Acknowledgements

The authors would like to thank M.Sc. Sebastian Schwaminger for his support during Raman spectroscopy. Dipl.-Ing. Cécile Boudot is gratefully acknowledged for her assistance during material processing. We thank Prof. Sebastian Günther (Specific field Physical Chemistry with Focus on Catalysis Faculty of Chemistry, Technische Universität München) for the use of the XPS and Raman devices.

Declaration of Conflicting Interests

The author(s) declared no potential conflicts of interest with respect to the research, authorship, and/or publication of this article.

Funding

The author(s) received no financial support for the research, authorship, and/or publication of this article.

References

- Jain A, Duvvuri LS, Farah S, et al. Antimicrobial polymers. *Adv Healthc Mater* 2014; 3: 1969–1985.
- DeQueiroz G and Day DF. Antimicrobial activity and effectiveness of a combination of sodium hypochlorite and hydrogen peroxide in killing and removing *Pseudomonas aeruginosa* biofilms from surfaces. *J Appl Microbiol* 2007; 103: 794–802.
- Dixon RE, Kaslow RA, Mackel DC, et al. Aqueous quaternary ammonium antiseptics and disinfectants use and misuse. *■ ■ ■*; 21: 2415–2417.
- Rutala W and Weber DJ. Uses of inorganic hypochlorite (bleach) in health-care facilities. *Clin Microbiol Rev* 1997; 10: 597–610.
- Bastarrachea L, Dhawan S and Sablani SS. Engineering properties of polymeric-based antimicrobial films for food packaging: a review. *Food Eng Rev* 2011; 3: 79–93.
- Fisher LE, Hook AL, Ashraf W, et al. Biomaterial modification of urinary catheters with antimicrobials to give long-term broadspectrum antibiofilm activity. *J Control Release* 2015; 202: 57–64.
- Kowalczyk D, Ginalska G, Piersiak T, et al. Prevention of biofilm formation on urinary catheters: comparison of the sparfloxacin-treated long-term antimicrobial catheters with silver-coated ones. *J Biomed Mater Res Part B Appl Biomater* 2012; 100 B: 1874–1882.
- Sawada I, Fachrul R, Ito T, et al. Development of a hydrophilic polymer membrane containing silver nanoparticles with both organic antifouling and antibacterial properties. *J Memb Sci* 2012; 387–388: 1–6.
- Rahaman MS, Thérien-Aubin H, Ben-Sasson M, et al. Control of biofouling on reverse osmosis polyamide membranes modified with biocidal nanoparticles and antifouling polymer brushes. *J Mater Chem B* 2014; 2: 1724–1732.
- Muñoz-Bonilla A and Fernández-García M. Polymeric materials with antimicrobial activity. *Prog Polym Sci* 2012; 37: 281–339.
- Dallas P, Sharma VK and Zboril R. Silver polymeric nanocomposites as advanced antimicrobial agents: classification, synthetic paths, applications, and perspectives. *Adv Colloid Interface Sci* 2011; 166: 119–135.
- Wu J, Boström P, Sparks LM, et al. Beige adipocytes are a distinct type of thermogenic fat cell in mouse and human. *Cell* 2012; 150: 366–376.
- Pauksch L, Hartmann S, Rohnke M, et al. Biocompatibility of silver nanoparticles and silver ions in primary human mesenchymal stem cells and osteoblasts. *Acta Biomater* 2014; 10: 439–449.

14. Greulich C, Kittler S, Epple M, et al. Studies on the biocompatibility and the interaction of silver nanoparticles with human mesenchymal stem cells (hMSCs) Langenbecks. *Arch Surg* 2009; 394: 495.
15. Siedenbiedel F and Tiller JC. Antimicrobial polymers in solution and on surfaces: overview and functional principles. *Polymers (Basel)* 2012; 4: 46–71.
16. Lansdown ABG. A pharmacological and toxicological profile of silver as an antimicrobial agent in medical devices. *Adv Pharmacol Sci* 2010; 2010: 1–16.
17. Tran QH, Nguyen VQ and Le A-T. Silver nanoparticles: synthesis, properties, toxicology, applications and perspectives. *Adv Nat Sci Nanosci Nanotechnol* 2013; 4: 033001.
18. Egerton TA and Tooley IR. Effect of changes in TiO₂ dispersion on its measured photocatalytic activity. *J Phys Chem B* 2004; 108: 5066–5072.
19. Tong T, Binh CTT, Kelly JJ, et al. Cytotoxicity of commercial nano-TiO₂ to *Escherichia coli* assessed by high-throughput screening: effects of environmental factors. *Water Res* 2013; 47: 2352–2362.
20. Banerjee S, Gopal J, Muraleedharan P, et al. Physics and chemistry of photocatalytic titanium dioxide: visualization of bactericidal activity using atomic force microscopy. *Current* 2006; 90: 1378–1383.
21. Lin B, Luo Y, Teng Z, et al. Development of silver/titanium dioxide/chitosan adipate nanocomposite as an antibacterial coating for fruit storage. *LWT Food Sci Technol* 2015; 63: 4–11.
22. Chung CJ, Tsou HK, Chen HL, et al. Low temperature preparation of phase-tunable and antimicrobial titanium dioxide coating on biomedical polymer implants for reducing implant-related infections. *Surf Coat Technol* 2011; 205: 5035–5039.
23. Chen C-C, Wang C-C and Yeh J-T. Improvement of odor elimination and anti-bacterial activity of polyester fabrics finished with composite emulsions of nanometer titanium dioxide-silver particles-water-borne polyurethane. *Text Res J* 2010; 80: 291–300.
24. Zhang X, Su H, Zhao Y, et al. Antimicrobial activities of hydrophilic polyurethane/titanium dioxide complex film under visible light irradiation. *J Photochem Photobiol A Chem* 2008; 199: 123–129.
25. Huppmann T, Yatsenko S, Leonhardt S, et al. Antimicrobial polymers – the antibacterial effect of photoactivated nano titanium dioxide polymer composites. *AIP Conference Proceedings* 2014; 440: 440–443.
26. Huppmann T. Maximierung der Oberflächentoxizität von Polymeren durch Titandioxid. ■■ 2014; 126 S: Available at: <https://mediatum.ub.tum.de/doc/1221765/1221765.pdf>.
27. Shit SC and Shah P. A review on silicone rubber. *Natl Acad Sci Lett* 2013; 36: 355–365.
28. DIN 52980:2008. Deutsches Institut für Normung e.V. Photokatalytische Aktivität von Oberflächen – Bestimmung der photokatalytischen Aktivität durch Abbau von Methylenblau.
29. DIN 55660:2011. Deutsches Institut für Normung e.V. Bestimmung der freien Oberflächenenergie fester Oberflächen durch Messung des Kontaktwinkels.
30. DIN 13697:2015. Deutsches Institut für Normung e. V. Chemische Desinfektionsmittel und Antiseptika – Quantitativer Oberflächen-Versuch nicht poröser Oberflächen zur Bestimmung der bakteriziden und/oder fungiziden Wirkung chemischer Desinfektionsmittel in den Bereichen Lebensmittel, Industrie, Haus.
31. Wagner CD, Riggs WM, Davis LE, et al. *Handbook of X-ray photoelectron spectroscopy*. Minnesota: Perkin-Elmer Corp., Physical Electronics Division, 1981.
32. Armanyanov S, Stankova NE, Atanasov PA, et al. XPS and μ -Raman study of nanosecond-laser processing of poly(dimethylsiloxane) (PDMS). *Nucl Instrum Methods Phys Res Sect B Beam Interact Mater Atoms* 2015; 360: 30–35.
33. Schnyder B, Lippert T, Kötz R, et al. UV-irradiation induced modification of PDMS films investigated by XPS and spectroscopic ellipsometry. *Surf Sci* 2003; 532–535: 1067–1071.
34. Rigby SJ, Al-Obaidi AHR, Lee S-K, et al. The application of Raman and anti-stokes Raman spectroscopy for in situ monitoring of structural changes in laser irradiated titanium dioxide materials. *Appl Surf Sci* 2006; 252: 7948–7952.
35. Cai D, Neyer A, Kuckuk R, et al. Raman, mid-infrared, near-infrared and ultraviolet–visible spectroscopy of PDMS silicone rubber for characterization of polymer optical waveguide materials. *J Mol Struct* 2010; 976: 274–281.
36. Yan X, Ohno T, Nishijima K, et al. Is methylene blue an appropriate substrate for a photocatalytic activity test? A study with visible-light responsive titania. *Chem Phys Lett* 2006; 429: 606–610.
37. Xu N, Shi Z, Fan Y, et al. Effects of particle size of TiO₂ on photocatalytic degradation of methylene blue in aqueous suspensions. *Ind Eng Chem Res* 1999; 38: 373–379.
38. Novotná P, Zita J, Krýsa J, et al. Two-component transparent TiO₂/SiO₂ and TiO₂/PDMS films as efficient photocatalysts for environmental cleaning. *Appl Catal B Environ* 2008; 79: 179–185.
39. Lee S-K and Mills A. Novel photochemistry of leuco-Methylene Blue. *Chem Commun* 2003; 18: 2366–2367.
40. Zhang L and Yu JC. A simple approach to reactivate silver-coated titanium dioxide photocatalyst. *Catal Commun* 2005; 6: 684–687.
41. Piera E, Ayllón J, Doménech X, et al. TiO₂ deactivation during gas-phase photocatalytic oxidation of ethanol. *Catal Today* 2002; 76: 259–270.
42. Youn B-H and Huh C-S. Surface characterization of silicone polymer used as an outdoor insulator by the measurement of surface voltage decay. *Surf Interface Anal* 2002; 33: 954–959.
43. Zhu Y, Otsubo M, Honda C, et al. Loss and recovery in hydrophobicity of silicone rubber exposed to corona discharge. *Polym Degrad Stab* 2006; 91: 1448–1454.
44. Oláh A, Hillborg H and Vancso GJ. Hydrophobic recovery of UV/ozone treated poly(dimethylsiloxane): adhesion studies by contact mechanics and mechanism of surface modification. *Appl Surf Sci* 2005; 239: 410–423.
45. Fujishima A, Rao TN and Tryk DA. Titanium dioxide photocatalysis. *J Photochem Photobiol C Photochem Rev* 2000; 1: 1–21.